Journal of Marine Science and Technology
https://doi.org/10.1007/s00773-024-01035-x

ORIGINAL ARTICLE

Validation of theoretical estimation methods and maximum value distribution calculation for parametric roll amplitude in long-crested irregular waves

Keiji Katsumura[1] · Leo Dostal[2] · Taiga Kono[1] · Yuuki Maruyama[1] · Masahiro Sakai[1] · Atsuo Maki[1]

Received: 27 March 2024 / Accepted: 25 October 2024

Abstract
Parametric rolling is a parametric excitation phenomenon caused by GM variation in waves. There are a lot of studies of the estimation the conditions, the occurrence, and the amplitude of parametric rolling. On the other hand, there are relatively few cases in which theoretical methods for estimating parametric roll amplitudes in irregular waves have been validated in tank tests. The primary objective of this study is to validate theoretical estimation methods for the parametric roll amplitude in irregular waves and improve their accuracy. First, the probability density functions (PDF) of the parametric roll amplitude obtained from the model ship motion experiment in irregular waves are compared with that obtained from theoretical estimation methods. Second, the method to improve the accuracy of estimation of the roll restoring variation in irregular waves is suggested. Third, the method to estimate the distribution of the maximum amplitude of parametric rolling in irregular waves. As a result, the PDFs of the roll amplitude obtained from the experiments differ from the results of theoretical estimation. After that, by correcting GM variation, the results of theoretical estimation are closer to the experimental results. Moreover, by the theoretical estimation method using the moment equation, the qualitative estimation for the PDF of the maximum roll amplitude is succeeded.

Keywords Model test · Probability density function · Grim's effective wave concept · Moment equation · Extreme value · GM variation

1 Introduction

Parametric rolling is a parametric excitation phenomenon caused by GM variation in waves. It is particularly likely to occur on container ships, whose transom stern and bow flare cause significant changes in the secondary moment of the waterline near the stern of the ship. For example, the accident of a C11 class container ship caused by parametric rolling in 1998 is well known [1]. Moreover, the accident of a pure car and truck carrier (PCTC) also occurred in recent years [2]. To prevent such dangerous phenomenon, parametric rolling, it is necessary to estimate its conditions, occurrence, and amplitude.

1.1 Related research

There is a long research history on theoretical estimation methods for the conditions, the occurrence, and the amplitude of parametric rolling. The parametric rolling in regular seas has been theoretically explored by Kerwin [3], Zavodney et al. [4], Francescutto [5], Bulian [6], Spyrou [7], Umeda et al. [8], Maki et al. [9], and Sakai et al. [10]. Furthermore, in particular, since the 1980s, there have been a lot of studies on theoretical estimation methods for parametric rolling in irregular waves. In order to study parametric rolling in irregular waves, systems excited by colored noise must be treated. One of methods to treat such systems theoretically is through a probabilistic approach. Spyrou [7], Dostal [11] and Maki [12] discussed the occurrence of parametric rolling in terms of the stability of the origin of the system with parametric excitation due to the roll restoring

✉ Keiji Katsumura
katsumura_keiji@naoe.eng.osaka-u.ac.jp

[1] Department of Naval Architecture and Ocean Engineering, Graduate School of Engineering, Osaka University, 2-1 Yamadaoka, Suita, Osaka, Japan

[2] Institute of Mechanics and Ocean Engineering, Hamburg University of Technology, 21043 Hamburg, Germany

Published online: 22 November 2024

variation in irregular waves. Furthermore, Belenky et al. [13] showed that the parametric roll motion is non-ergodic and not normal. Mohamad and Sapsis [14] derived an analytical approximation to the probability density function (hereinafter referred to as PDF) for the non-Gaussian response of Mathieu's equation under parametric excitation using the probabilistic decomposition-synthesis method [15]. Maki et al. [16] suggested the estimation method for determining the non-Gaussian PDF of the parametric roll angle in irregular wave introducing the nonlinear damping coefficient. For the estimation of parametric roll amplitudes, studies using stochastic averaging methods have been conducted. Using the stochastic averaging method, Roberts [17] derived the stochastic differential equation

for a phase and an amplitude. In Roberts' results, the PDF of the roll amplitude was obtained, which was modeled using a cubic restoring component and damping. Subsequently, Roberts et al. [18, 19] proposed an energy based methodology and attempted to reflect the restoring component. Dostal et al. [20] proposed an energy-based stochastic averaging method using the Hamiltonian. Furthermore, Maruyama et al. [21] extended the method from [20]. They compared the results of Roberts [17] and Dostal [20]'s methods with those of Monte Carlo Simulation (hereinafter referred to as MCS). As a result, they reported a discrepancy in the tail of the PDF and proposed a method called the Simulation-Based Stochastic Averaging Method to solve the discrepancy. In addition, Maruyama et al. [22] proposed a method for estimating parametric rolling using the moment equation [23] (hereinafter referred to as the moment method). This method also allows to obtain some quantitative agreement with the result of MCS for the PDF of the parametric roll amplitude [24]. On the other hand, there are relatively few cases in which these analytical methods for estimating roll motion have been validated in tank tests.

Moreover, estimation of the roll restoring variation is important in the theoretical estimation of parametric rolling. In the studies of the theoretical estimation of parametric rollong in irregular waves by Maruyama et al. [21, 22, 24] mentioned above, the roll restoring variation was estimated by considering only the wave component based on the Froude-Krylov assumption under quasi-statically balancing heave and pitch in waves and introducing Grim's effective wave concept [25]. However, Hashimoto et al. [26] suggest that the estimation method of the roll restoring variation considering only the wave component based on the Froude-Krylov assumption under quasi-statically balancing heave and pitch in waves might overestimate the risk of parametric rolling due to the large roll restoring variation during wave passage through the captive model test. Yu et al. [27] compare the degree of this overestimation using five models that estimate nonlinear restoring forces and Froude–Krylov forces. Furthermore, Hashimoto et al. [28] measured the roll restoring variation in a captive model test in irregular waves and compared it with the results of the calculation of the roll restoring variation using Grim's effective wave. The results suggested that the accuracy of the roll restoring variation using Grim's effective wave remained a problem.

1.2 Object and scope

The primary objective of this study is to validate theoretical estimation methods for the parametric roll amplitude in irregular waves and improve their accuracy. The contributions of this study are as follows:

1. Validation of theoretical estimation methods for parametric roll amplitude by comparison with corresponding experimental result,
2. Suggestion for the method to improve the accuracy of estimation of the roll restoring variation in irregular waves, and
3. Suggestion for the method to estimate the distribution of the maximum amplitude of parametric rolling in irregular waves.

In this study, we first conducted the model ship motion experiment in order to obtain the PDF of parametric roll amplitude in long-crested irregular waves in the towing tank of Osaka University. After that, the accuracy of the theoretical methods is validated by comparing the experimental results with the PDFs of the parametric roll amplitude calculated using three theoretical calculation methods; Roberts' stochastic averaging method [17], the energy-based stochastic averaging method [20] (hereinafter referred to as ESAM), and the moment method [22, 24].

Furthermore, we attempted to improve the accuracy of the theoretical estimation method by using the equation of motion reflecting the correction of the roll restoring variation based on the captive model test by Kono et al.

Extreme value theory [29] is also widely used in risk assessment in various engineering fields. Extreme value theory was introduced by McTaggart [30], McTaggart and de Kat [31] in ship motion. From the perspective of risk assessment for parametric rolling, it would be significant to introduce the idea of extreme value theory and estimate the maximum parametric roll amplitude. On the other hand, accurate estimation of the distribution of maximum values requires accurate estimation of the PDF of the parametric rolling amplitude down to the tail. For estimating the tail of the distribution of roll motion, an approach using the peaks-over-threshold method has been studied by Glotzer et al. [32] and Pipiras [33]. Belenky et al. [34] analyzed the tail part of the PDF for application to probabilistic estimation of the extreme values of the roll motion. Anastopoulos and Spyrou [35] proposed a new framework for modeling the tail

Table 1 Principal particulars of C11 at model and full scale

Items	Value	
Scale	Model	Full
L_{pp} (m)	2.62	262
B (m)	0.4	40
D (m)	0.2445	24.45
d (m)	0.115	11.5
W (kg)	67.247	6.7247×10^7
C_b	0.56	0.56
GM (m)	0.019299	1.9299
T_ϕ (s)	2.44	24.4

part of the distribution of the roll motion, using generalized Pareto distribution. Belenky et al. [36] also applied extreme value theory to estimate the probability of the occurrence of capsizing using the split-time method.

In the present study, we pay particular attention to the behavior of the tail section of the PDF of the parametric roll amplitude in order to estimate extreme values. Finally, we propose a method for calculating the distribution of the maximum roll amplitude based on the theoretical method.

2 Subject ship

The subject ship is a C11 class post-Panamax container ship. In this study, a geometric similarity model with a scale of 1/100 is used for model tests at the towing tank of Osaka University. The main features of the model are shown in Table 1. The extinction coefficients used in the calculations were calculated from the results of free-rolling tests using the model in a water tank.

3 Towing tank experiment

By conducting model ship motion experiments in long-crested irregular waves and obtaining the PDF of the roll amplitude, we validate the theoretical calculation method as described in Sect. 1. This section describes the experimental method used in this study.

The bow and stern of the model ship is connected to the towing dolly with a rubber strap to gently restrain the model ship. The tension of the rubber strap was adjusted appropriately so as not to constrain the surge or roll motion too much. The stern rubber strap was not used in most of the experiments in head-wave conditions. The state of the model ship is shown in Fig. 1. The setup of the experiment is shown in Fig. 2. The long-crested irregular head waves are generated using ITTC spectrum. The instantaneous rolling of the model ship is measured by a fiber-optic gyro sensor mounted at the center of gravity of the model ship. Wave elevations of irregular waves are measured by a wave level gauge installed at the front of the model ship. Wave heights are computed from time series of measured wave elevations. The experimental conditions for irregular waves are shown in Table 2. The producing time for each irregular wave is 300 s at model scale. Here, considering the arrival time of waves from the wave generator and the effect of reflected waves, the data measured by the gyro sensor between 270 s from 70 s to 340 s at model scale after the start of producing waves were considered for the analysis.

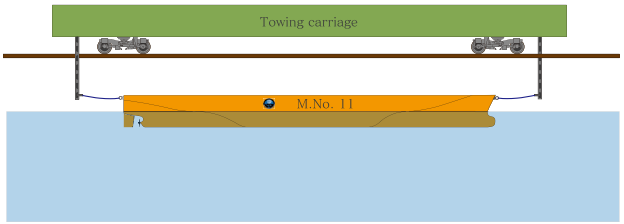

Fig. 1 Schematic view of the experiment

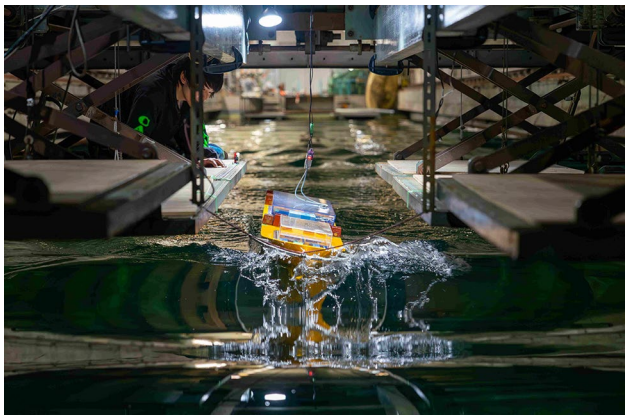

Fig. 2 The situation of the experiment

Table 2 Wave condition at full scale

Items	Value	
$H_{1/3}$ (m)	5.0	7.0
T_{01} (s)	10.0	10.0
Num. of realizations	24	24

4 Experimental results and discussion

4.1 Analysis methods and theoretical estimation methods for roll amplitudes

An example of a time series of the roll angle obtained in the experiment is shown in Fig. 3.In this study, the following two methods of analyzing the roll amplitude are used.

4.1.1 Experimental zero crossing method

In the time series data of the roll angle obtained in the experiment, The time series data of roll angle is obtained by the experiment. The maximum value between every zero up crossing and zero down crossing and the minimum value between every zero down crossing and zero up crossing are recorded. The absolutes of them are the roll amplitudes.

The PDF is calculated from the distribution of the obtained roll amplitudes.

4.1.2 Experimental envelope method

The Hilbert transform of the time series of roll angles obtained in the experiment is used to create an envelope. Using the Hilbert transform [37, 38], the analytical signal of the real data can be derived, its instantaneous amplitude and instantaneous phase can be obtained, and the envelope can be created. In the stochastic averaging method [17, 20] described in Sect. 4.2, the amplitude is obtained from the instantaneous roll angle values, not the local maxima and minima, as in the analysis method using the Hilbert transform based envelope. Considering this feature, the analysis method using the envelope of the Hilbert transform was introduced in this study in order to compare the results of the stochastic averaging method with experimental results. Then, the absolute value of the envelope of the roll angle at each sampling point is recorded as the amplitude. The PDF is calculated from the distribution of the values of roll angles.

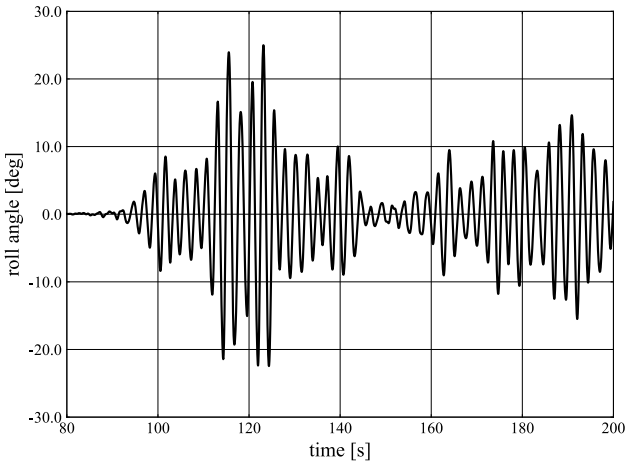

Fig. 3 Time history of roll angle, $H_{1/3} = 7.0$ m, $T_{01} = 10.0$ s

4.2 Theoretical estimation methods

Theoretical estimation of the amplitude of parametric rolling in irregular waves requires the estimation of the corresponding the roll restoring variation. In this study, we focus on the GM variation in waves as a factor that reflects the variation of the stability in waves, and use the following one-degree-of-freedom roll motion equation.

$$\frac{\mathrm{d}^2\phi}{\mathrm{d}t^2} + b_1\frac{\mathrm{d}\phi}{\mathrm{d}t} + b_2\frac{\mathrm{d}\phi}{\mathrm{d}t}\left|\frac{\mathrm{d}\phi}{\mathrm{d}t}\right| + b_3\left(\frac{\mathrm{d}\phi}{\mathrm{d}t}\right)^3 + \sum_{n=1}^{5} a_{2n-1}\phi^{2n-1} + P(t)\phi = M_{\mathrm{w}}(t) \tag{1}$$

$$P(t) = \frac{\omega_0^2}{GM_0}GM(t) \tag{2}$$

In Eq. 1, ϕ is the roll angle. b_1, b_2, and b_3 are the linear, quadratic, and cubic damping coefficients divided by I_{xx}, where I_{xx} is the moment of inertia in roll including the corresponding added moment of inertia. The coefficients of the polynomial approximation of the GZ curve are a_i ($i = 1, 3, 5, 7,$ and 9), $M_{\mathrm{w}}(t)$ is the moment related to waves. The GM variation term is $P(t)$, which can be expressed by Eq. 2. Moreover, ω_0 is the natural roll frequency, and GM_0 is the metacentric height in still water. However, the GM variation in waves is complicated and not always clearly defined [39]. Therefore, in this study, we introduce Grim's effective wave theory [25] for irregular waves. Moreover, considering only the wave component based on the Froude-Krylov assumption under quasi-statically balancing heave and pitch in waves, we obtain an equation relating the displacement of the wave at the center of the hull to the amount of GM variation [21, 22]. This relationship is called the non-memory transformation. In this way, we estimate GM variation in irregular waves. The specific procedure of this transformation method is described in detail in "Appendix" section.

Based on the roll restoring variation estimated in this way, we estimate the amplitude of parametric rolling in irregular waves using three theoretical methods, Roberts' stochastic averaging method [17], ESAM [20], and the moment method [24].

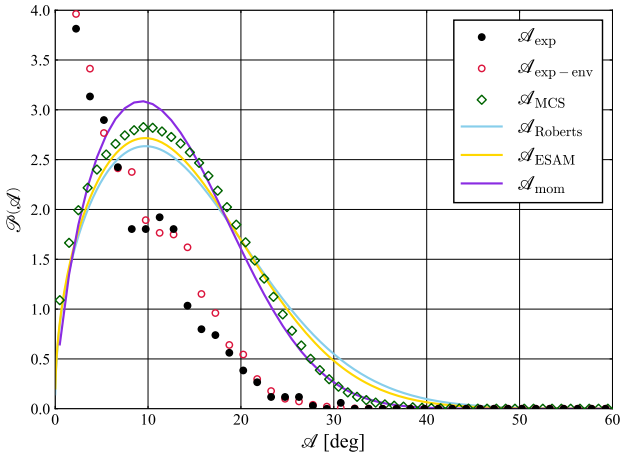

Fig. 4 PDF of roll amplitude, $H_{1/3} = 5.0$ m, $T_{01} = 10.0$ s, linear scale

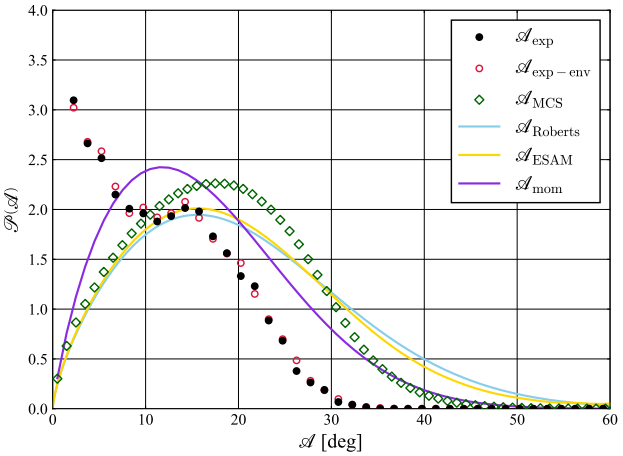

Fig. 6 PDF of roll amplitude, $H_{1/3} = 7.0$ m, $T_{01} = 10.0$ s, linear scale

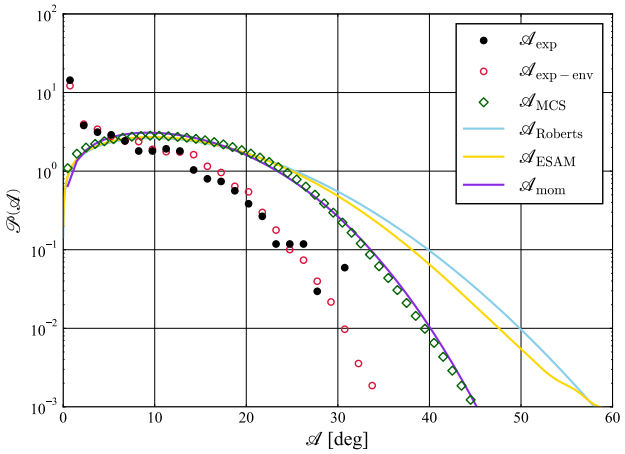

Fig. 5 PDF of roll amplitude, $H_{1/3} = 5.0$ m, $T_{01} = 10.0$ s, logarithmic scale

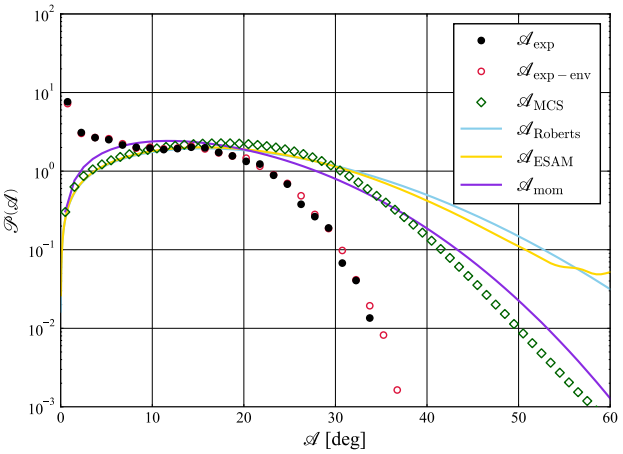

Fig. 7 PDF of roll amplitude, $H_{1/3} = 7.0$ m, $T_{01} = 10.0$ s, logarithmic scale

4.3 Experimental and theoretical results

The results of comparing the PDFs of the roll amplitudes obtained from experiments and various theoretical calculation methods are shown in Figs. 4, 5, 6 and 7. Here, the black dots in the figure are the PDF calculated by the experimental zero crossing method described in Sect. 4.1.1 and the red dots are the PDF calculated by the experimental envelope method described in Sect. 4.1.2. The cyan line is the PDF obtained by Roberts' stochastic averaging method [17], the yellow line is the PDF obtained by ESAM [20], and the purple line is the PDF obtained by the moment method [24]. The green diamonds are the PDF obtained by MCS. For MCS, the initial value of the roll angle was set to 5 deg, and the initial value of the roll velocity was set to 0 deg/s. The time for one trial of simulation was 3600 s. The number of trials was 10^4 times.

4.4 Consideration

From Figs. 4, 5, 6 and 7, the PDFs obtained by the experimental zero crossing method described in Sect. 4.1.1 are almost equal to those obtained by the experimental envelope method described in Sect. 4.1.2. Therefore the authors conclude that the results of both experimental analysis methods could be used in terms of comparing the PDFs obtained by theoretical estimation methods and those of experimental results. On the other hand, the PDFs of the roll amplitudes obtained from the experiments differ quantitatively and qualitatively from the PDFs obtained from the simulation

and from each theoretical prediction method. Around 0 deg, the simulation and theoretical results show that the PDF converges to 0, while the experimental results are non-zero. The experimental values have a local maximum from 10 to 20 deg, and then they are smaller than the theoretical values. In the experiments, an intermittent rolling behavior was observed, whereas pure parametric rolling behavior resulted from the theoretical methods and the MCS of the equations of motion. In Figs. 6 and 7, the form of the PDF from the experiments obtained here, which takes non-zero values around 0 deg and has one more hump in the range of 10–20 deg, is not consistent with the two forms of the theoretical PDFs presented in previous studies [24, 40]. We currently believe that the reason for such PDFs is the change of yaw angle during the experiment. In the experiment, the model ship was gently strained by a rubber strap so as not to constrain the surge or roll motion too much. However, the yaw motion could not be completely restrained. Further investigation is necessary in the future. Moreover, the sample size of the experiment in this study was 6480 s for a total of 270 s times 24 at model scale. The sample size may not be sufficient to discuss the tail of the PDF obtained from experiments. Further discussion on increasing sample size and the appropriate amount of sample size are needed in the future.

Next, we compare the three PDFs obtained by the theoretical method with that obtained by MCS. In Fig. 6, the PDFs obtained by Roberts' stochastic averaging method and ESAM agree well with the result obtained by MCS in the amplitude range from 0 deg to 10 deg.

However, in the log scale in Fig. 7, the PDF obtained by the moment method agrees better with the result of MCS in the tail (large amplitude part) of the PDF. As mentioned in Sect. 1, the estimation of the maximum roll amplitude requires an accurate estimation of the PDF of the roll amplitude down to the tail part. Therefore, when consider the PDF of the maximum roll amplitude in Sect. 6 using theoretical methods, the results obtained by the moment method, which are successful in quantitatively estimating the tail, are considered more suitable for use in Eq. 5.

5 Correction of GM variation

As shown in Figs. 6 and 7, there was a discrepancy between the experimental PDF and the PDF obtained by MCS and each theoretical calculation. We attempt to reduce this discrepancy in order to improve the estimation accuracy of the PDF of the parametric roll amplitude. One way to consider the stability in waves is to focus on GM variation. On the other hand, GM variation in waves is complicated and not always clearly defined [39]. In this study, GM variation is calculated by the equation relating wave displacement and GM variation. We consider only the wave component based on the Froude-Krylov assumption under quasi-statically balancing heave and pitch in waves, and introduce Grim's effective wave theory [25] for irregular waves as explained in Sect. 4.2 [21, 22]. The equation relating the wave elevation at amidship to the GM variation is called the non-memory transformation. The specific calculation procedure is described in "Appendix" section. However, the results of captive model tests in regular following waves by Hashimoto et al. [26] suggests that the estimation method of the roll restoring variation considering only the wave component based on the Froude-Krylov assumption under quasi-statically balancing heave and pitch in waves might overestimate the risk of parametric rolling due to the large roll restoring variation during wave passage. Furthermore, Hashimoto et al. [28] measured the roll restoring variation in a captive model test in irregular waves and compared it with the results of the calculation of the roll restoring variation using Grim's effective wave. The results suggest that the accuracy of the roll restoring variation using Grim's effective wave remains a problem. Therefore, we consider the accuracy of the estimation of the roll restoring variation to be one of the reasons for the discrepancy between the experimental and theoretical results for the PDF of the parametric roll amplitude in irregular waves. Hence, captive model tests were conducted to evaluate the estimation accuracy of the theoretical equation for GM variation.

5.1 Captive model test

The experimental method for the captive model testing is explained in the following. The setup of this experiment is shown in Fig. 8. The difference from the experiment Fig. 2, in which the model ship was restrained by the rubber strap described in Sect. 3, is that the model ship in the captive model test experiment was restrained by the heaving rod. The model ship was free to heave and pitch, and was attached to the towing vehicle via a quarter force

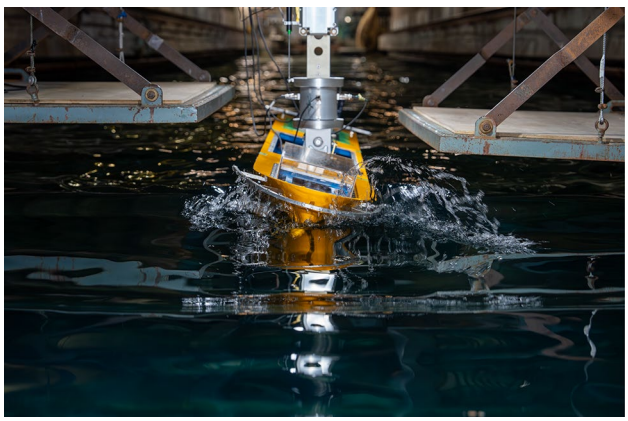

Fig. 8 Condition during captive model test

Table 3 Wave condition at full scale on the captive model test

Items	Value		
$H_{1/3}$ (m)	5.0	5.0	7.0
T_{01} (s)	10.0	12.37	10.0
Num. of realizations	10	10	10

gauge. The fore-and-aft force (F_X), lateral force (F_Y), turning moment (N), lateral tilting moment (K), heaving, and pitching on the hull were measured. In addition, irregular waves were generated by a flap wave generator at the end of the tank, and the generated irregular wave forms were measured using a capacitance type water level gauge installed between the wave generator and the model ship. Three wave conditions were used in this experiment, see Table 3. For each wave condition, the number of realizations is 10.In the experiment of this study, the fixed roll angles ϕ were 0, 5, 10, and 15 degrees. The GM variation ΔGM was obtained from the difference between the roll moment at $\phi = 0$ deg.

5.2 Experimental result and method of correcting GM variation

The theoretical PDF is calculated based on ΔGM(t) created in "Appendix" section. The experimental PDF and theoretical PDFs are shown in Figs. 9 and 10. The black line is the experimental value and the blue line is the theoretical value based on the relation Eq. 9. In Fig. 9 and 10, the non-normality was shown in the experimental and theoretical PDFs of GM variation. Maruyama et al. [22] also revealed

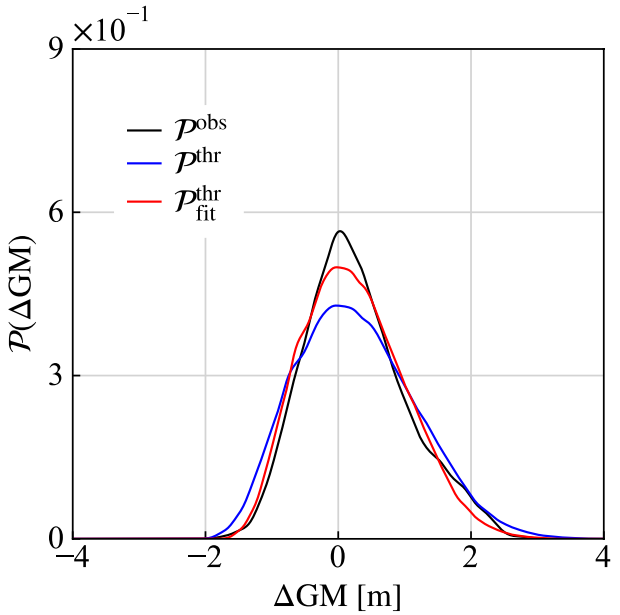

Fig. 9 PDF of ΔGM with $H_{1/3} = 0.07$ m, $T_{01} = 1.0$ s, linear scale

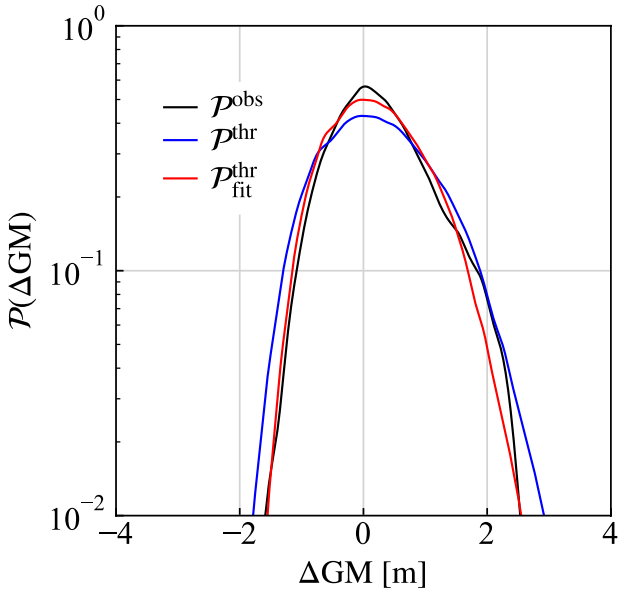

Fig. 10 PDF of ΔGM with $H_{1/3} = 0.07$ m, $T_{01} = 1.0$ s, logarithmic scale

the absence of normality of the PDF of GM variation in irregular wave in the simulation using the same subject ship. This asymmetry might be an inherent property of the PDF of GM variation in waves. Further research about this non-normality could be necessary. By comparison, the theoretical PDF has a wider range of ΔGM than the experimental PDF. Therefore, it is found that the conventional theoretical PDFs are overestimated compared to the experimental PDFs. Therefore, to improve the PDF of the roll amplitude obtained by theoretical methods such that it reproduces the experimental results, we attempt to correct the theoretical GM variation. In this study, although Figs. 9, 10 and Maruyama et al. [22] showed absence of normality in GM variation, as the simplest approximation, we assume that ΔGM is normally distributed. With this we correct Eq. 9 as Eq. 3 using the ratio of the standard deviation $\sigma_{\mathrm{GM}}^{\mathrm{obs}}$ of the experimental values to the standard deviation $\sigma_{\mathrm{GM}}^{\mathrm{thr}}$ of the theoretical values. In Figs. 9 and 10, the red line is the theoretical value based on Eq. 3.

$$\Delta\mathrm{GM}(\zeta_{\mathrm{mid}}) = \frac{\sigma_{\mathrm{GM}}^{\mathrm{obs}}}{\sigma_{\mathrm{GM}}^{\mathrm{thr}}} \sum_{k=0}^{6} \mathrm{C_k} \zeta_{\mathrm{mid}}^{\mathrm{k}} \tag{3}$$

5.3 Calculation results of parametric rolling amplitude

The conventional equation of motion for one-degree-of-freedom roll motion is shown in Eq. 1.

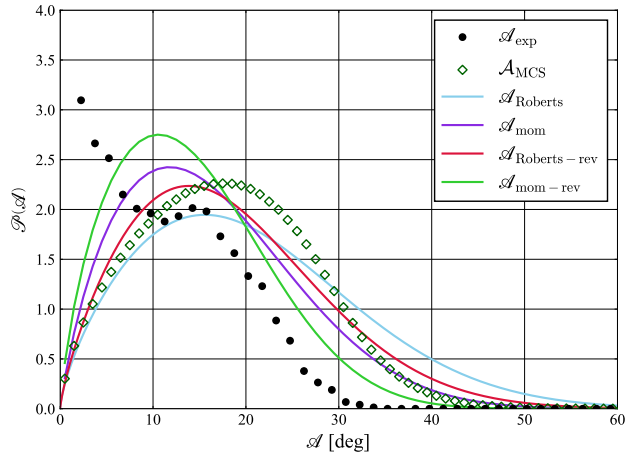

Fig. 11 Comparison of the PDFs of the roll amplitude before and after correction, $H_{1/3} = 7.0$ m, $T_{01} = 10.0$ s, linear scale

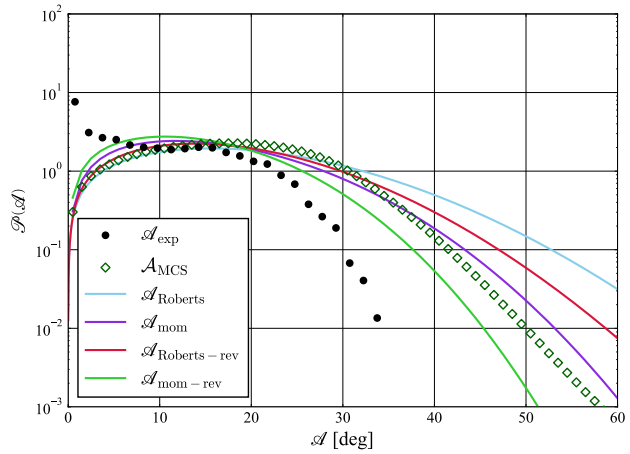

Fig. 12 Comparison of PDF of roll amplitude before and after correction, $H_{1/3} = 7.0$ m, $T_{01} = 10.0$ s, logarithmic scale

According to Sect. 5.2, we multiplied the modification coefficient $\sigma_{\mathrm{GM}}^{\mathrm{obs}}/\sigma_{\mathrm{GM}}^{\mathrm{thr}}$ by $P(t)$. The final equation of motion is given by

$$\frac{\mathrm{d}^2\phi}{\mathrm{d}t^2} + b_1\frac{\mathrm{d}\phi}{\mathrm{d}t} + b_2\frac{\mathrm{d}\phi}{\mathrm{d}\bar{t}}\left|\frac{\mathrm{d}\phi}{\mathrm{d}t}\right| + b_3\left(\frac{\mathrm{d}\phi}{\mathrm{d}t}\right)^3 + \sum_{n=1}^{5} a_{2n-1}\phi^{2n-1} + \frac{\sigma_{\mathrm{GM}}^{\mathrm{obs}}}{\sigma_{\mathrm{GM}}^{\mathrm{thr}}}P(t)\phi = M_{\mathrm{w}}(t). \tag{4}$$

Applying Roberts stochastic averaging method [17] and the moment method [24] to the equations of motion Eq. 1 and Eq. 4 before and after correction, respectively, the PDFs of the roll amplitude are obtained. These theoretical PDFs are compared with the PDF obtained from the experiment in Figs. 11 and 12. The black dots denote the experimental result, the cyan line and the red line are the theoretical results obtained by Roberts' stochastic averaging method before and after correction, and the purple line and the green line are the theoretical results obtained by the moment method before and after correction. The green diamonds are the PDF obtained by MCS.

The results of Figs. 11 and 12 show that the calculation results after the correction of the GM variation are closer to the experimental results than before the correction, and the accuracy of the quantitative estimation of the roll amplitude is improved. However, there is still a large difference between the experimental and theoretical results, mainly due to the discrepancy in the region of small roll angles. Our theoretical method using the corrected equation of motion could not completely represent an intermittent rolling behavior as in the experiments. Therefore, further improvement of the used model equations and the theoretical calculation methods is desirable, such as introducing an additive yaw disturbance or external forces. In this study, Grim's effective wave [25] and the non-memory transformation [21, 22] were used to estimate the GM variation. However, roll restoring variation in waves is complicated [39] and challenges remain in estimating and correcting the GM variation approach. In addition, in this study, the GM variation in waves is corrected by assuming a normal distribution and using standard deviations although the non-normality is known [22]. Even under this assumption, the theoretical results of PDFs of the parametric roll amplitudes were improved, as shown in Figs. 11 and 12. However, further research is needed to evaluate the influences of the normality assumption, and to investigate and model the non-normality of the GM variation.

6 PDF of the maximum roll amplitude

In order to estimate the distribution of the maximum values of the parametric roll amplitude, a theoretical expression for the PDF of the maximum roll amplitude is derived. The PDF of the maximum roll amplitude is then estimated based on the PDF obtained by the moment method, which is in quantitative agreement with the MCS results in Sect. 4. Moreover, the PDF estimated by the theoretical method is compared with the results of MCS in order to confirm the accuracy of the estimation of the PDF of the maximum roll amplitude.

When the extreme values such as the maximum of parametric roll amplitude are treated, the presence or absence of the independence of the data is important [29, 41]. On the other hand, strictly speaking, roll amplitudes are self-dependent [42]. It is also known that this dependence can be strong for the case of large roll amplitude, and decorrelation time in the case of parametric roll can be long [43]. However, in this study, we assume that the roll amplitudes are independent as the simplest approximation because the

distribution of the maxima for the parametric roll is not clear and the PDFs of the roll amplitudes are obtained using the theoretical methods in Sect. 4. The distribution of the maxima of roll amplitudes is derived from the PDF of the roll amplitudes.

6.1 Derivation of a theoretical formula to estimate the PDF of the maximum roll amplitude

Suppose now that N_0 amplitudes are extracted from the population of roll amplitudes and the highest value among them is $\mathscr{A}_{\mathrm{M}}$, where $\mathscr{A}_{\mathrm{M}}$ is a dimensionless value. Denoting the PDF of $\mathscr{A}_{\mathrm{M}}$ as $\mathscr{P}^*\left(\mathscr{A}_{\mathrm{M}}\right)$, the probability that the maximum value of the amplitude $\mathscr{A}$ is in $[\mathscr{A}_{\mathrm{M}},\ \mathscr{A}_{\mathrm{M}}+\mathrm{d}\mathscr{A}_{\mathrm{M}}]$ is $\mathscr{P}^*\left(\mathscr{A}_{\mathrm{M}}\right)\mathrm{d}\mathscr{A}_{\mathrm{M}}$.

This is the probability that only one of the N_0 amplitudes is between $\mathscr{A}_{\mathrm{M}}$ and $\mathscr{A}_{\mathrm{M}}+\mathrm{d}\mathscr{A}_{\mathrm{M}}$ and the remaining $\left(N_0-1\right)$ amplitudes are less than $\mathscr{A}_{\mathrm{M}}$. Thus $\mathscr{P}^*\left(\mathscr{A}_{\mathrm{M}}\right)$ can be expressed as follows Eq. 5 [44]

$$\mathscr{P}^*\left(\mathscr{A}_{\mathrm{M}}\right)\mathrm{d}\mathscr{A}_{\mathrm{M}} = N_0\left[1-\int_{\mathscr{A}_{\mathrm{M}}}^{\infty}\mathscr{P}(\mathscr{A})\mathrm{d}\mathscr{A}\right]^{N_0-1} \mathscr{P}\left(\mathscr{A}_{\mathrm{M}}\right)\mathrm{d}\mathscr{A}_{\mathrm{M}} \tag{5}$$

where $\mathscr{P}\left(\mathscr{A}_{\mathrm{M}}\right)$ is the value of PDF when the amplitude $\mathscr{A}$ is $\mathscr{A}_{\mathrm{M}}$.

From the above, $\mathscr{P}^*\left(\mathscr{A}_{\mathrm{M}}\right)$, the PDF of the maximum roll amplitude, is obtained.

Also, when N_0 is large enough, i.e., $N_0 \to \infty$, then

$$\xi = N_0\int_{\mathscr{A}_{\mathrm{M}}}^{\infty}\mathscr{P}(\mathscr{A})\mathrm{d}\mathscr{A} \tag{6}$$

$$\lim_{N_0\to\infty}\left[1-\int_{\mathscr{A}_{\mathrm{M}}}^{\infty}\mathscr{P}(\mathscr{A})\mathrm{d}\mathscr{A}\right]^{N_0} = \lim_{N_0\to\infty}\left[1-\frac{\xi}{N_0}\right]^{N_0} = e^{-\xi} \tag{7}$$

Therefore, Eq. 5 can be expressed in terms of Eq. 8.

$$\mathscr{P}^*\left(\mathscr{A}_{\mathrm{M}}\right)\mathrm{d}\mathscr{A}_{\mathrm{M}} = \xi e^{-\xi}\left[\int_{\mathscr{A}_{\mathrm{M}}}^{\infty}\mathscr{P}(\mathscr{A})\mathrm{d}\mathscr{A}\left\{1-\int_{\mathscr{A}_{\mathrm{M}}}^{\infty}\mathscr{P}(\mathscr{A})\mathrm{d}\mathscr{A}\right\}\right]^{-1} \mathscr{P}\left(\mathscr{A}_{\mathrm{M}}\right)\mathrm{d}\mathscr{A}_{\mathrm{M}} \tag{8}$$

6.2 Calculation method

The specific procedure for the calculation of the PDF of the maximum roll amplitude using MCS and theoretical method based on Eq. 5 is explained as follows. The initial value of the roll angle on MCS is set to 5 deg, and

the first N_0 amplitudes are extracted from the time series data of the roll angle after 500 s from the start of the simulation. The maximum value among the N_0 amplitudes is recorded as the maximum value in one trial. By repeating this N times,

N maximum values are obtained in total. Based on these N maxima, the PDF of the maximum roll amplitude is calculated.

Then, the shapes of each PDF with N_0 as the variable are compared.

On the other hand, $\mathscr{P}(\mathscr{A})$, the PDF of the roll amplitude, is calculated using the moment method and Roberts' stochastic averaging method. Using this, the PDF of the maximum roll amplitude is theoretically derived by using Eq. 5. Then, the PDF of the maximum roll amplitude calculated by the theoretical method is compared with that obtained from the MCS results.

6.3 Numerical results

With $N_0 = 20,\ 50,\ 10^2,\ 10^3,\ 10^4$, the PDFs of the maximum roll amplitude calculated by MCS are shown in Figs. 13 and 14. When $N_0 = 20,\ 50,\ 10^2,\ 10^3$, the number of MCS trials N is 10^4. When $N_0 = 10^4$, N is 5×10^3.

The results calculated by Eq. 5 using the moment method and Roberts' stochastic averaging method are compared with that obtained from MCS and are shown in Figs. 15, 16, 17,18, 19 and 20.

6.4 Discussion and limitations

From Figs. 13 and 14, it can be seen that as N_0 increases, the peak of the PDF moves to the right and the range becomes narrower. As N_0 increases, the number of samples for searching the maximum value per trial increases. Therefore, a

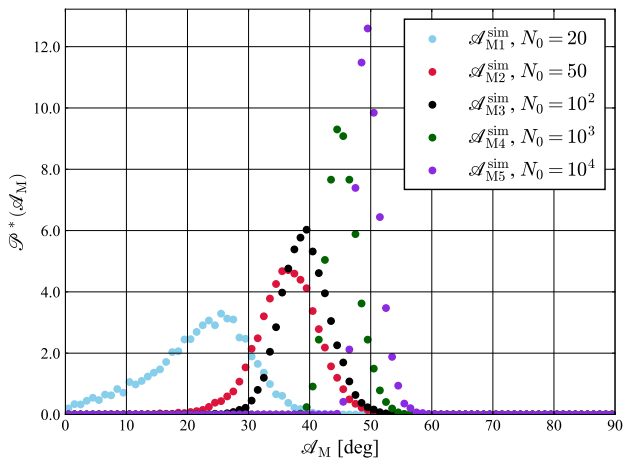

Fig. 13 PDF of the maximum of roll amplitudes obtained by MCS, $H_{1/3} = 7.0$ m, $T_{01} = 10.0$ s, linear scale

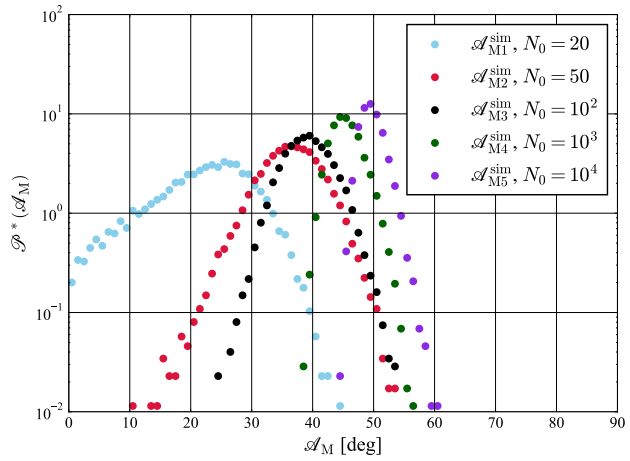

Fig. 14 PDF of the maximum of roll amplitudes obtained by MCS, $H_{1/3} = 7.0$ m, $T_{01} = 10.0$ s, logarithmic scale

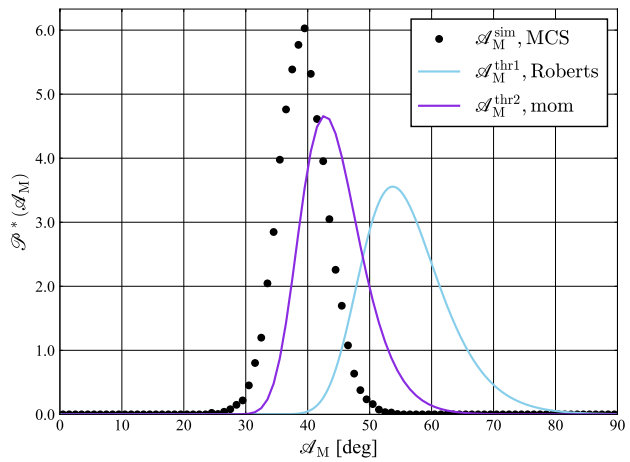

Fig. 15 Comparison of PDF of the maximum of roll amplitudes obtained theoretical method and MCS, $H_{1/3} = 7.0$ m, $T_{01} = 10.0$ s, $N_0 = 10^2$, linear scale

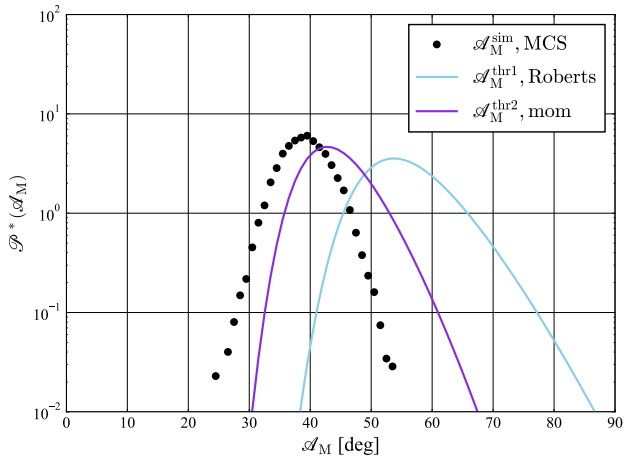

Fig. 16 Comparison of PDF of the maximum roll amplitudes obtained by the theoretical methods and MCS, $H_{1/3} = 7.0$ m, $T_{01} = 10.0$;s, $N_0 = 10^2$, logarithmic scale

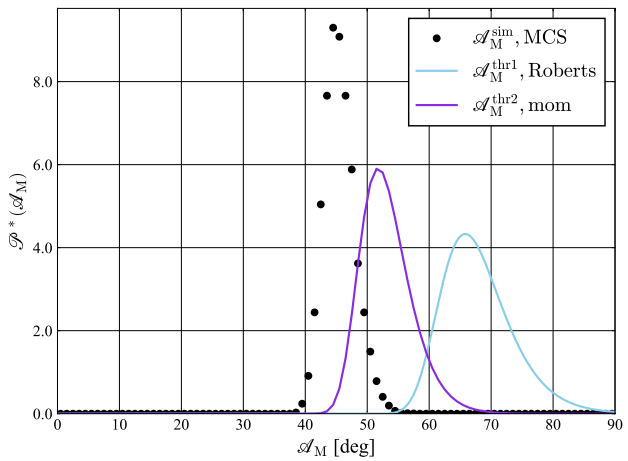

Fig. 17 Comparison of PDF of the maximum roll amplitudes obtained by the theoretical methods and MCS, $H_{1/3} = 7.0$ m, $T_{01} = 10.0$ s, $N_0 = 10^3$, linear scale

larger value is counted as the maximum value per trial, and the peak moves to the right. The fact that the shape of the PDF changes with N_0 suggests that we need to pay attention to the number of samples N_0 per trial when estimating the maximum value. It is also known that, if the sample size is sufficiently large, the distribution of maxima of independent samples converges to three types of distributions: the Gumbel distribution, the Fréchet distribution, and the Weibull distribution [45, 46]. The distribution of the maximal amplitudes of parametric rolling may also need to be examined in terms of its convergence and the type of the converged distribution, which is a topic for future research by the authors.

Also, looking at the Figs. 15 and ,16, in terms of the position of the peak, the result obtained by the moment method is in better agreement with the result of MCS than that by Roberts' stochastic averaging method. This may be due to the accuracy of the estimation of the tail of the PDF of the roll amplitude by the theoretical calculation, as mentioned in Sect. 4.4. Therefore, it can be concluded that the moment method provides a better qualitative result for the PDF of the maximum roll amplitude. On the other hand, under conditions where N_0 is large, the deviation between the theoretical value and the MCS result becomes large, and the estimation accuracy remains somewhat problematic. In the future, it may be necessary to improve the theoretical estimation method of the PDF of the roll amplitude.

Moreover, Eq. 5 was derived by assuming independence of the parametric roll amplitudes. On the other hand, it is

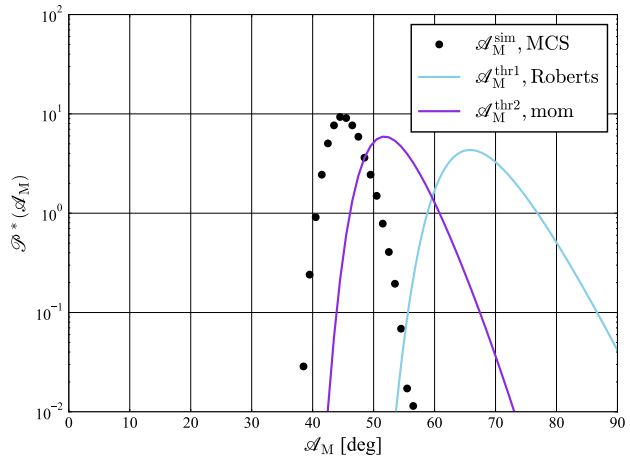

Fig. 18 Comparison of PDF of the maximum roll amplitudes obtained by the theoretical methods and MCS, $H_{1/3} = 7.0$ m, $T_{01} = 10.0$ s, $N_0 = 10^3$, logarithmic scale

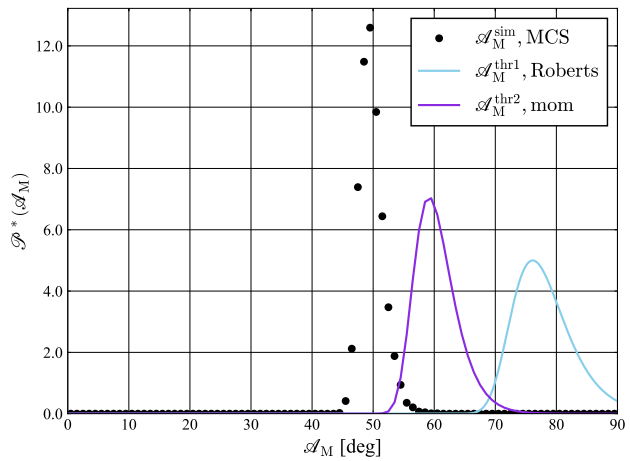

Fig. 19 Comparison of PDF of the maximum roll amplitudes obtained by the theoretical methods and MCS, $H_{1/3} = 7.0$ m, $T_{01} = 10.0$ s, $N_0 = 10^4$, linear scale

known that the roll amplitudes are self-dependent [42]. It may be necessary in the future to evaluate the influence of the assumption of independence of roll amplitudes and to develop theoretical methods that reflect this self-dependence.

7 Conclusion

The accuracy of the PDF estimation of the parametric roll amplitude in long-crested irregular waves was validated by comparing the results of each theoretical method with the experimental results. In this study, the experimental results were generally smaller, especially after 20 deg, and differed from the results of each theoretical method. In the tail

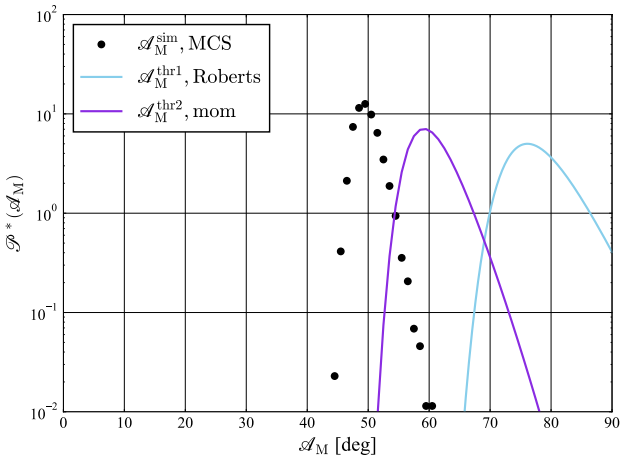

Fig. 20 Comparison of PDF of the maximum roll amplitudes obtained by the theoretical methods and MCS, $H_{1/3} = 7.0$ m, $T_{01} = 10.0$ s, $N_0 = 10^4$, logarithmic scale

section of the PDF, the PDF result of the moment method is smaller than those obtained by Roberts' stochastic averaging method and ESAM. Therefore, in the considered cases, the moment method is the most suitable for extreme value estimation. The experimental PDF of the roll amplitude had a shape with humps and hollows, in the range of 10 to 20 deg in Figs. 6 and 7. We believe that this is due to the change in the yaw angle in the experiment. Further study is needed to develop a model which introduces an additional yaw disturbance and also to improve the experimental method.

To further improve the theoretical estimation methods for the PDF of parametric roll amplitude, the authors attempted to correct the estimated GM variation. In Figs. 11 and 12, although the PDF using the corrected GM variation and the equation of motion approached the PDF obtained by the experimental results, a notable difference still remains between the theoretical and experimental results. The roll restoring variation in waves is complicated [39], and further development of modeling and theoretical methods is desirable, as well as the estimation and correction of the GM variation. In this study, the theoretical GM variation was corrected by assuming a normal distribution and using standard deviations although the non-normality of GM variation was shown in Figs. 9 and 10. The influence of this assumption or the evaluation and modeling of the non-normality of the GM variation needs to be investigated in further research.

Then, the PDFs of the maximum roll amplitude were calculated using the moment method and Roberts' stochastic averaging method, and the results were compared with that using the MCS. The results showed that the moment method gave a better agreement with the MCS results than Roberts' stochastic averaging method, and that the maximum value

could be estimated quantitatively. However, it was also confirmed that the deviation from the MCS results becomes larger when N_0 is large. We conclude that more accurate estimation of the PDF of the parametric roll amplitude is needed to resolve this issue. Moreover, in this study, independence of roll amplitudes was assumed. Evaluation of the influence of this assumption and development of theoretical methods that reflect this self-dependence may be necessary in the future.

Appendix: Method of the estimation of GM variation

Procedure for calculating GM variation

The following procedure is used to calculate the GM variation (ΔGM) in irregular waves.

1. Generation of time series for Grim's effective wave
2. Equation relating wave elevation and GM Variation
3. Generation of time series of GM variation

Each calculation method is explained following.

Grim's effective wave concept

This is the calculation method performed in Item 3. Grim's effective wave is the replacement of a spatially irregular waveform around a ship by a single regular wave using the least-squares method, and this regular wave is called the effective wave [25]. As in Fig. 21, this effective wave is assumed to have a wavelength to ship length ratio of 1, and the crest or trough of the wave is in the center of the hull. The amplitude of this effective wave has a linear relationship with ocean wave displacement, while the effect of the wave on the righting lever has a nonlinear and non-memory relationship. As a result, there are no major obstacles to the statistical treatment of the GM variation in irregular waves. The time series of the effective wave displacement $\zeta_{\mathrm{Grim}}(t)$ is calculated by using the ocean wave spectrum $S(\omega)$.

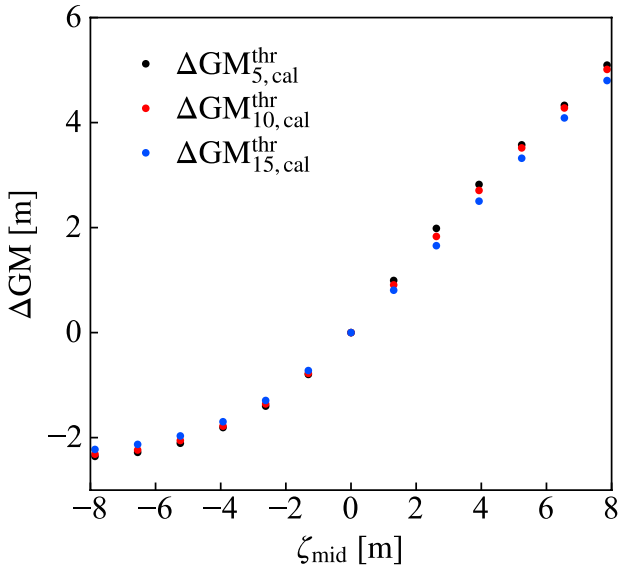

Fig. 22 The relationship between ΔGM and ζ_{mid}

Two methods for generating the time series of effective wave is presented by Maruyama et al. [22]. One method is based on the superposition of component waves [Method 1] [25], and the other is based on the application of a linear filter [Method 2] [22]. In this study, in Sects. 4 and 6, Method 1 was used on Roberts' stochastic averaging method and ESAM, and Method 2 was used on MCS and the moment method. In Sect. 5, Method 1 was used.

Method of non-memory transformation

This is the calculation method performed by Item 2. The non-memory transformation is obtained by the relationship between wave elevation and GM variation at amidship. Considering only the wave component based on the Froude-Krylov assumption under quasi-statically balancing heave and pitch in waves, we obtain the equation relating wave displacement and GM variation [21, 22] in regular waves with the ratio of the wavelength to the ship length of 1. The wave peaks and troughs are assumed to always exist in the center of the hull. Using the numerical

Fig. 21 The schematic view of Grim's effective wave

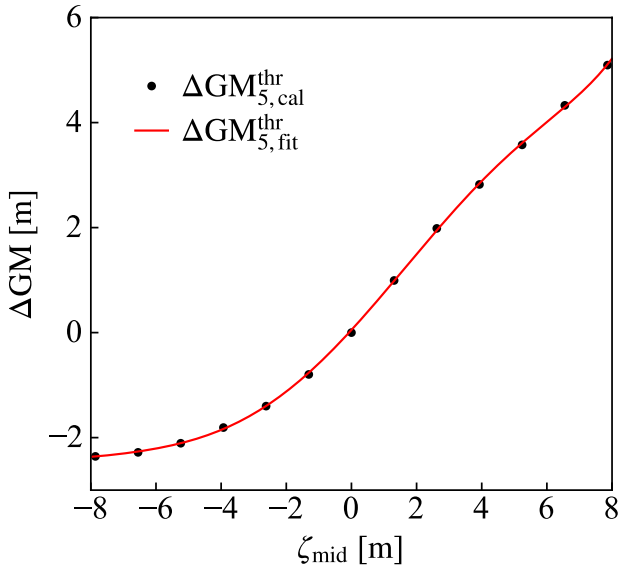

Fig. 23 The polynomial approximation of the relationship between ΔGM and ζ_{mid}

simulation, we calculate the GM variation $\Delta GM^{thr}_{\phi,cal}$ when the regular wave peaks and troughs are located in the center of the hull and the heel angle of the hull is ϕ [deg] for each wave elevation ζ_{mid}. The restoring arm is calculated from hydrodynamic theory [47, 48]. As a result, the relationship diagram in Fig. 22 is obtained. Where the wave displacement is positive when the wave trough is located in the center of the hull and it is negative when the wave crest is located in the center of the hull. The original data is plotted by the black dotted line in Fig. 22. The sixth-order polynomial approximation of the original data is used to obtain a curve of GM variation for arbitrary wave displacements. The red dotted line in Fig. 23 is the result of the polynomial approximation of the original data as in Eq. 9, where $N_p = 6$. Using this relation given by Eq. 9 between the wave displacement at the center of the hull and the GM variation, the time series of the effective wave displacement calculated in Item 1 is transformed into the time series of the GM variation.

$$\Delta GM^{thr}_{\phi,fit}(\zeta_{mid}) = \sum_{k=0}^{N_p} C_k \zeta_{mid}^k \tag{9}$$

Acknowledgements This study was supported by a Grant-in-Aid for Scientific Research from the Japan Society for the Promotion of Science (JSPS KAKENHI Grant #22H01701). The authors would like to thank the referees for their detailed comments, helpful advice, and suggestions.

Funding Open Access funding provided by Osaka University.

Data availability The authors did not agree for their data to be shared publicly. Therefore, data is not available.

References

1. France WN, Levadou M, Treakle TW, Paulling JR, Michel RK, Moore C (2003) An investigation of head-sea parametric rolling and its influence on container lashing systems. Mar Technol SNAME News 40(1):1
2. Rosén A, Huss M, Palmquist M (2012) Experience from parametric rolling of ships. In: Parametric resonance in dynamical systems, pp 147–165
3. Kerwin JE (1955) Notes on rolling in longitudinal waves. Int Shipbuild Prog 2(16):597
4. Zavodney LD, Nayfeh A, Sanchez N (1989) The response of a single-degree-of-freedom system with quadratic and cubic nonlinearities to a principal parametric resonance. J Sound Vib 129(3):417
5. Francescutto A (2001) An experimental investigation of parametric rolling in head waves. J Offshore Mech Arct Eng 123(2):65
6. Bulian G (2004) Approximate analytical response curve for a parametrically excited highly nonlinear 1-dof system with an application to ship roll motion prediction. Nonlinear Anal Real World Appl 5(4):725
7. Spyrou K (2005) Design criteria for parametric rolling. Ocean Eng Int 9(1):11
8. Umeda N, Hashimoto H, Vassalos D, Urano S, Okou K (2004) Nonlinear dynamics on parametric roll resonance with realistic numerical modelling. Int Shipbuild Prog 51(2–3):205
9. Maki A, Umeda N, Shiotani S, Kobayashi E (2011) Parametric rolling prediction in irregular seas using combination of deterministic ship dynamics and probabilistic wave theory. J Mar Sci Technol 16(3):294
10. Sakai M, Umeda N, Yano T, Maki A, Yamashita N, Matsuda A, Terada D (2018) Averaging methods for estimating parametric roll in longitudinal and oblique waves. J Mar Sci Technol 23(3):413
11. Dostal L, Kreuzer E, Sri Namachchivaya N (2012) Non-standard stochastic averaging of large-amplitude ship rolling in random seas. Proc R Soc A Math Phys Eng Sci 468(2148):4146
12. Maki A, Maruyama Y, Liu Y, Dostal L (2024) Comparison of stochastic stability boundaries for parametrically forced systems with application to ship rolling motion. J Mar Sci Technol 29:446
13. Belenky VL, Weems KM, Lin WM, Paulling JR (2011) Probabilistic analysis of roll parametric resonance in head seas. Contemp Ideas Ship Stab Capsizing Waves 97:555
14. Mohamad MA, Sapsis TP (2016) Probabilistic response and rare events in Mathieu's equation under correlated parametric excitation. Ocean Eng 120:289

15. Mohamad MA, Cousins W, Sapsis TP (2016) A probabilistic decomposition-synthesis method for the quantification of rare events due to internal instabilities. J Comput Phys 322:288
16. Maki A, Sakai M, Umeda N (2019) Estimating a non-gaussian probability density of the rolling motion in irregular beam seas. J Mar Sci Technol 24:1071
17. Roberts JB (1982) Effect of parametric excitation on ship rolling motion in random waves. J Ship Res 26(4):246
18. Roberts JB, Spanos PD (1986) Stochastic averaging: an approximate method of solving random vibration problems. Int J Non-Linear Mech 21(2):111
19. Roberts JB, Vasta M (2000) Markov modelling and stochastic identification for nonlinear ship rolling in random waves. Philos Trans R Soc Lond A 358:1917
20. Dostal L, Kreuzer E (2011) Probabilistic approach to large amplitude ship rolling in random seas. Proc Inst Mech Eng C J Mech Eng Sci 225(10):2464
21. Maruyama Y, Maki A, Dostal L, Umeda N (2022) Improved stochastic averaging method using Hamiltonian for parametric rolling in irregular longitudinal waves. J Mar Sci Technol 27(1):186
22. Maruyama Y, Maki A, Dostal L, Umeda N (2022) Application of linear filter and moment equation for parametric rolling in irregular longitudinal waves. J Mar Sci Technol 27:1252
23. Bover DCC (1978) Moment equation methods for nonlinear stochastic systems. J Math Anal Appl 65(2):306
24. Maruyama Y, Maki A, Dostal L (2024) Probability density function of roll amplitude for parametric rolling using moment equation. J Mar Sci Technol 29:641–655
25. Grim O (1961) Beitrag zu dem problem der sicherheit des schiffes im seegang. Schiff und Hafen (in German) 6:490
26. Hashimoto H, Umeda N (2004) Nonlinear analysis of parametric rolling in longitudinal and quartering seas with realistic modeling of roll-restoring moment. J Mar Sci Technol 9:117
27. Yu L, Ma N, Wang S (2019) Parametric roll prediction of the kcs containership in head waves with emphasis on the roll damping and nonlinear restoring moment. Ocean Eng 188:106
28. Hashimoto H, Umeda N, Sakamoto G, Bulian G (2006) Estimation of roll restoring moment in long-crested irregular waves. In: Conference Proceedings The Japan Society of Naval Architects and Ocean Engineers, vol 3, p 201
29. Coles S (2001) An introduction to statistical modeling of extreme values. Springer, London
30. McTaggart K (2000) Ongoing work examining capsize risk of intact frigates using time domain simulation. In: Contemporary ideas of ship stability, pp 587–595
31. McTaggart K, de Kat JO (2000) Capsize risk of intact frigates in irregular seas. Trans Soc Naval Archit Mar Eng 108:147
32. Glotzer D, Pipiras V, Belenky V, Campbell B, Smith T (2017) Confidence intervals for exceedance probabilities with application to extreme ship motion. Stat J 15(4):537
33. Pipiras V (2020) Pitfalls of data-driven peaks-over-threshold analysis: perspectives from extreme ship motions. Probab Eng Mech 60:103053
34. Belenky V, Glotzer D, Pipiras V, Sapsis TP (2019) Distribution tail structure and extreme value analysis of constrained piecewise linear oscillators. Probab Eng Mech 57:1
35. Anastopoulos PA, Spyrou KJ (2023) Effectiveness of the generalized pareto distribution for characterizing ship tendency for capsize. In: Contemporary ideas on ship stability, pp 245—263
36. Belenky V, Weems KJ, Lin WM, Pipiras V, Sapsis TP (2024) Estimation of probability of capsizing with split-time method. Ocean Eng 292:116452
37. Feldman M (2011) Hilbert transform in vibration analysis. Mech Syst Signal Process 25(3):735
38. King FW (2009) Hilbert transforms, vol 2. Cambridge Univ. Press, Cambridge
39. Belenky V, Weems KM (2008) Probabilistic qualities of stability change in waves. In: Proc. 10th Intl. Ship Stability Workshop, Daejon, Korea, pp 95–108
40. Maki A, Maruyama Y, Umeda U, Miino Y, Katayama T, Sakai M, Ueta T (2019) A perspective on theoretical estimation of stochastic nonlinear rolling. In: Proceedings of the 17th International Ship Stability Workshop, Helsinki, Finland, pp 39–46
41. Longuet-Higgins MS (1952) On the statistical distribution of the heights of sea waves. J Mar Res 6(3):245
42. Campbell B, Belenky V, Pipiras V, Weems K, Sapsis TP (2023) Estimation of probability of large roll angle with envelope peaks over threshold method. Ocean Eng 290:116296
43. Kim DH, Belenky V, Campbell B, Troesch AW (2014) Statistical estimation of extreme roll in head seas. In: Proceedings of the 33rd International Conference on Ocean, Offshore and Arctic Engineering OMAE 2014, San-Francisco, USA
44. Goda Y (2000) Random seas and design of maritime structures (Advanced Series on Ocean Engineering), vol 15. World Scientific Pub Co Inc, Singapore
45. Fisher RA, Tippet LHC (1928) Limiting forms of the frequency distribution of the largest or smallest member of a sample. Math Proc Camb Philos Soc 24(2):180–190
46. Gnedenko B (1943) Sur la distribution limite du terme maximum d'une série aléatoire. Ann Math 44(3):423
47. Umeda N, Yamakoshi Y (1992) Probability of ship capsizing due to pure loss of stability in quartering seas. Nav Archit Ocean Eng 30:73
48. Hamamoto M, Kim Y, Uwatoko K (1991) Study on ship motions and capsizing in following seas (final report). J Soc Nav Archit Jpn 170:173